# TOGA - a GNSS Reflections Instrument for Remote Sensing Using Beamforming

S. Esterhuizen, T.K. Meehan, D. Robison
Jet Propulsion Laboratory, California Institute of Technology
4800 Oak Grove Drive
Pasadena, CA, 91109
esterhui@jpl.nasa.gov

*Abstract*—Remotely sensing the Earth's surface using GNSS signals as bi-static radar sources is one of the most challenging applications for radiometric instrument design. As part of NASA's Instrument Incubator Program, our group at JPL has built a prototype instrument, TOGA (Time-shifted, Orthometric, GNSS Array), to address a variety of GNSS science needs. Observing GNSS reflections is major focus of the design/development effort. The TOGA design features a steerable beam antenna array which can form a high-gain antenna pattern in multiple directions simultaneously. Multiple FPGAs provide flexible digital signal processing logic to process both GPS and Galileo reflections. A Linux OS based science processor serves as experiment scheduler and data post-processor. This paper outlines the TOGA design approach as well as preliminary results of reflection data collected from test flights over the Pacific ocean. This reflections data demonstrates observation of the GPS L1/L2C/L5 signals.

### TABLE OF CONTENTS

1 INTRODUCTION ..... 1
2 ARCHITECTURE ..... 2
3 INSTRUMENT VERIFICATION ..... 2
4 CONCLUSIONS ..... 5
ACKNOWLEDGEMENTS ..... 5
REFERENCES ..... 5
BIOGRAPHY ..... 6

## 1. INTRODUCTION

Recently the use of GPS signals as opportunistic bistatic radar signals has become increasingly popular in the radar and navigation communities for remotely sensing the Earth surface[1]. A GPS bistatic radar uses two reception antennas: one tracking the direct signal from the satellite oriented skyward; the other observing the surface-reflected signal oriented toward the Earth (see Figure 1). Previous work in GPS bistatic radar includes using reflected signals to determine ocean roughness[2], soil moisture[3], and surface altimetry[4][5].

©2009 California Institute of Technology. Government sponsorship acknowledged.
IEEEAC Paper #1223, Version 4 Updated 03/19/2009.

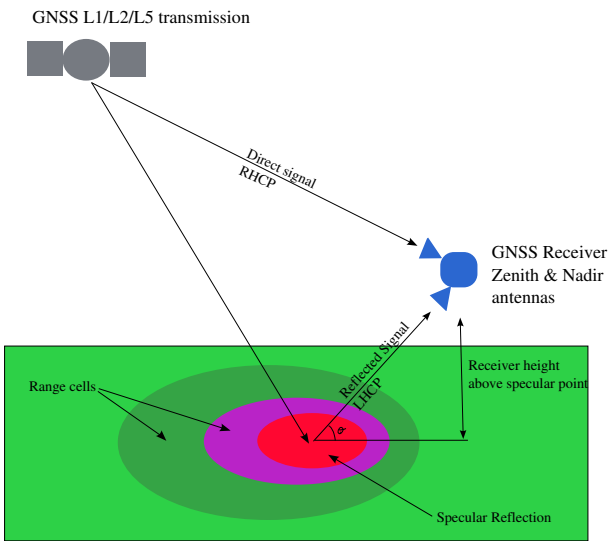


**Figure 1**. Bistatic radar concept. Direct signal always arrives first, reflected signal reverses polarization and arrives some time later

In all of the applications mentioned, these reflected signals are on average much weaker than the direct signal and in order to ensure high quality observations, a single element low-gain antenna might not suffice. This problem can be mitigated by using a high-gain antenna, but with the decreased field of view one can not observe multiple simultaneous reflections as with a lower gain antenna. The solution is to build up an antenna array with multiple lower-gain antennas, but to phase this array such that multiple simultaneous high-gain beams can be formed[6].

*Beamforming SNR Increase*

When beamforming with **N** antennas, the theoretical gain in voltage signal-to-noise ratio (SNRv) is expressed as the ratio of the increase in signal amplitude to the increase in noise. If **N** signals are added together, the amplitude increases by a factor of **N**. Assuming the noise is **independent** between signals, the RMS noise increases by $\sqrt{N}$, yielding a SNR increase of $\frac{N}{\sqrt{N}} = \sqrt{N}$.

## 2. ARCHITECTURE

The TOGA instrument consists of 5 major components (as illustrated in Figure 2):

- Antenna array
- RF Downconverters
- Reconfigurable Digital Processor (RDP)
- Real-time GNSS Receiver
- Science Processor

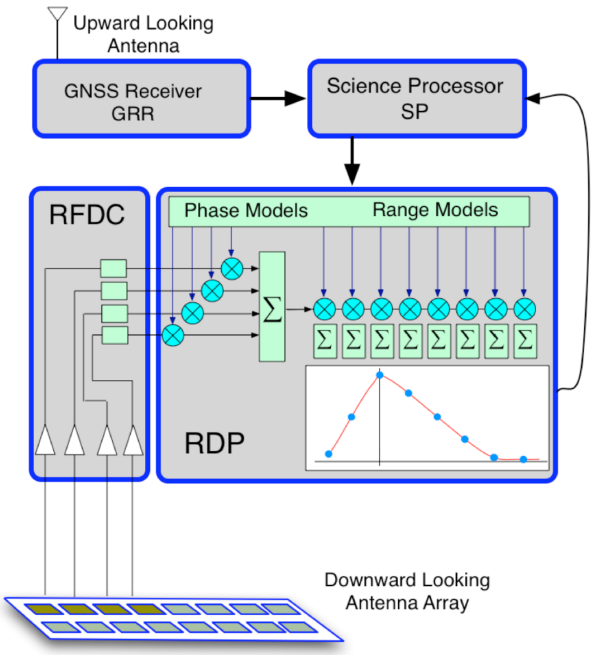


**Figure 2**. TOGA concept demonstrating all major instrument components. The science processor uses real-time data from the GNSS receiver to form models for pointing high-gain beams at the specular reflection points on Earth's surface

*Antenna Array*

The antenna array consists of:

- Antenna element
- L-band bandpass filter
- Low-noise Amplifier

It is worthwhile to note that with respect to beamforming, the array is completely passive. All beamforming is performed digitally at baseband in the Digital Processor.

TOGA is designed to accommodate a wide field of view (120 degrees) and support up to 16 antennas per baseband processor board at the three GNSS frequencies (L1, L2 and L5). These frequency bands cover both the GPS and Galileo frequency space.

*RF Downconverters*

Each wide-band RF signal is filtered and amplified then split into separate L1, L2 and L5 channels. The downconverter PCB supports up to 8 antennas, where each channel is downconverted with a single-stage mixer and low-pass filtered with a 10 MHz filter. This double side-band signal is then sampled with a 1-bit sampler at 20.456 MHz in quadrature producing two (I and Q) data streams resulting in 96 1-bit data streams for 3 frequencies and 8 antennas.

*Reconfigurable Digital Processor (RDP)*

These 96 1-bit datastreams are clocked into the RDP with a common 20.456 MHz sample clock and streamed to DDR memory. The memory can store up to 10 seconds of continuous observations. Once the observation period is complete, raw samples can be read back from memory at 4x the sample rate, which provides for a very flexible signal processing architecture: Now one can counter-rotate and correlate at different doppler frequencies and delays at leisure.

*Real-time GNSS Receiver*

A real-time GNSS receiver is used to track the direct signals, which is used to generate phase and delay models for off-line processing of the reflected data.

*Science Processor*

The science processor is a Linux computer that receives real-time tracking information from the GNSS Receiver and uses this information to form models for observing the reflected signal. In order to observe the reflected signal, the following parameters are required by the RDP:

- Which satellites are visible
- Observation start/stop time
- Direction to form beams in (Azimuth/Elevation) to maximize SNR
- Carrier and Code phase models

These parameters are sent to the RDP via a USB 2.0 interface, when the signal processing is completed, correlation waveforms can be downloaded from the RDP at up to 400 Mbps.

## 3. INSTRUMENT VERIFICATION

*Amplitude and Phase Stability Between Channels*

One of the first tests conducted on the hardware was checking stability of the amplitude and phase between 8 different RF channels. The experimental setup can be seen in Figure 3. A single tone at -110 dBm was passively split 8-ways, with 4 channels connected to the first RFDC board and the other 4 channels connected to another RFDC board. This way stability between boards and channels could be compared. The effect of a sudden temperature change was observed on the first day of the test around 17:00 by warming the RFDC boards up with a heat gun for a few seconds. The boards performed remarkably well, with relative phase varying only up to a few millicycles, while the amplitude change was nearly undetectable.

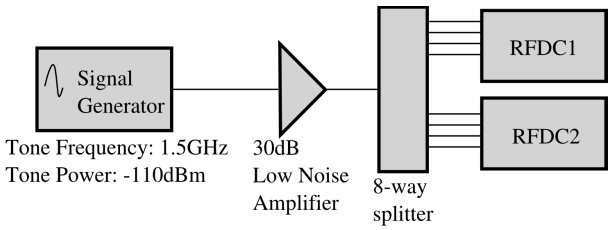


**Figure 3**. Experimental setup for amplitude and phase stability test. A tone at -110dbm was amplified and split 8 ways. 4 tones were downconverted and sampled at RFDC1, while the other 4 tones were downconverted and sampled at RFDC2. This way one can test stability between individual channels on the same board and stability between two different RFDC boards

Amplitude stability (Figure 4) seems very good, over two and a half days the amplitude didn't vary more than a few tenths of a dB. The relative amplitude between channels also appeared really well balanced, with RF channel 1 having the highest amplitude, while RF channel 6 had the lowest - both these channels were still within less than half a dB of each other.

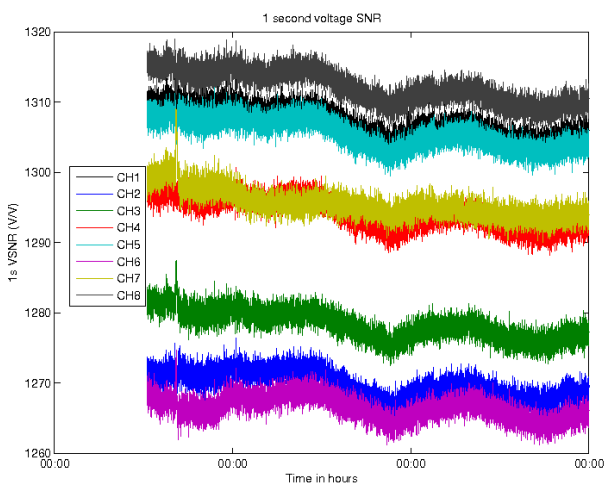


**Figure 4**. Amplitude stability over 2.5 days. All channels matched amplitude to less than half a dB.

The phase stability, plotted in Figure 5 indicates that the phase between channels and between RFDC boards do not vary more than a few milli-cycles over more than 2 days. This means that instrument delay calibration need only be done once.

*Lab Tests*

*Beamforming with pure tone*—The simplest method to test beamforming is to inject a tone into the RFDC then doing counter-rotation and accumulation of the samples. This setup is illustrated in Figure 6. To give the reader a better idea of what beamforming really does, examine Figure 7. The 8 low-amplitude sinusoids is the output of the accumulation process of each individual tone. Note how there is still a residual doppler left on the signal, this is because the phase model

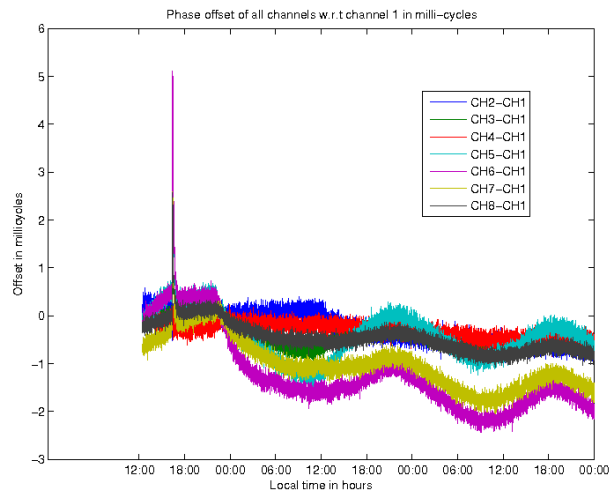


**Figure 5**. Phase stability over 2.5 days. The spike at 17:00 was caused by heating the RFDC boards up with a heat gun. Overall the relative phase didn't vary more than 2 millicycles over the data collection period.

wasn't perfect. Note also, how all 8 tones match in phase, this proves that beamforming worked correctly and signals can now be coherently added together resulting in an increase of SNR.

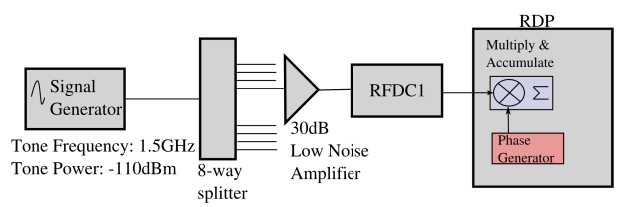


**Figure 6**. Setup for beamforming test using tones. The tone was split 8 ways and then amplified by 8 individual amplifiers. This was done to create independent noise at all 8 channels. After sampling the tones were counter-rotated with a phase model and accumulated over 1 millisecond

It is not enough to only examine the amplitudes of the beamformed signal, because with beamforming not only does the signal amplitude increase, the noise increases also.

| | Amplitude | Noise | 1ms SNR |
|---|---|---|---|
| a) 1 Antenna | 5920 | 161 | 37 |
| b) Beamformed | 47347 | 457 | 104 |
| $\frac{b}{a}$ increase | 7.997 | 2.84 | 2.81 |

**Table 1**. Amplitude and Noise values after 1ms of accumulation of a pure tone. Last row shows amplitude/noise/SNR increase of a beamformed signal over a single antenna signal

Theoretically when one beamformes with 8 antennas, the ex-

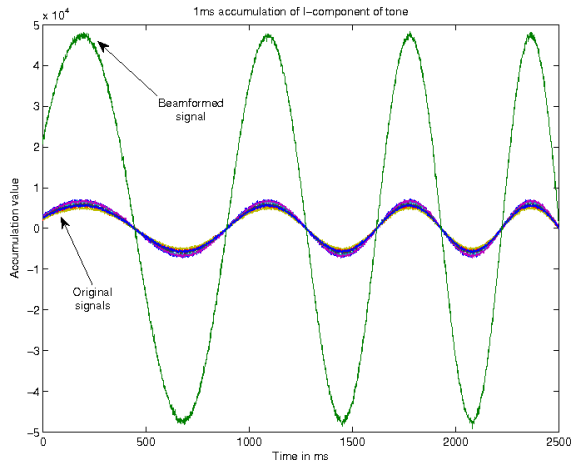


**Figure 7**. This plot shows the output of the I-component after phase counter-rotation and accumulation. Note that all 8 signals are coherent with respect to each other, meaning our beamforming is working correctly, adjusting the phase correctly for each antenna element to maximize SNR. After beamforming the resulting (higher amplitude) signal can be seen

pected SNR increase is $\sqrt{8} = 2.83$. According to Table 1, the increase was 2.81, which is within 0.06dB of the expected value.

*Beamforming with GPS*—Next, beamforming was conducted with 16 antennas observing the direct GPS signal at both L1 and L2 frequencies. Figure 8 shows the results after 3 simultaneous beams were formed and pointed at PRN1, PRN31 and PRN32. There is an obvious increase in signal amplitude, but again, one must carefully examine the RMS noise of the measurement - these results are provided in Table 2. From the table it is evident that the signal amplitude did indeed increase by a factor of 16, as expected, but the noise increased by 4.22 instead of $\sqrt{16} = 4$. This means that the noise at all 16 antennas were not completely independent, the authors suspect this could be due to RFI that is common to all the antennas. Even though the noise wasn't completely independent, beamforming with 16 antennas still yielded an increase in SNR by $20 \log \frac{114}{30} = 11.6dB$, within 0.5dB of the expected increase of $20 \log \sqrt{16} = 12$.

| | Amplitude | Noise | 1ms SNR |
|---|---|---|---|
| a) 1 Antenna | 5580 | 186 | 30 |
| b) Beamformed | 89310 | 785 | 114 |
| $\frac{b}{a}$ increase | 16 | 4.22 | 3.8 |

**Table 2**. Amplitude and Noise values after 1ms of accumulation of L1 C/A PRN31. Last row shows amplitude/noise/SNR increase of a beamformed signal over a single antenna signal

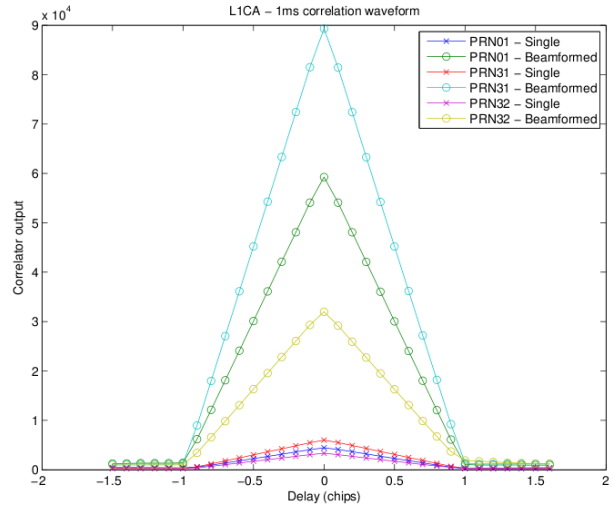


**Figure 8**. RSS of correlation waveform before and after L1 beamforming. Three simultaneous beams were formed pointing at PRN1,PRN31 and PRN32 with 16 antennas

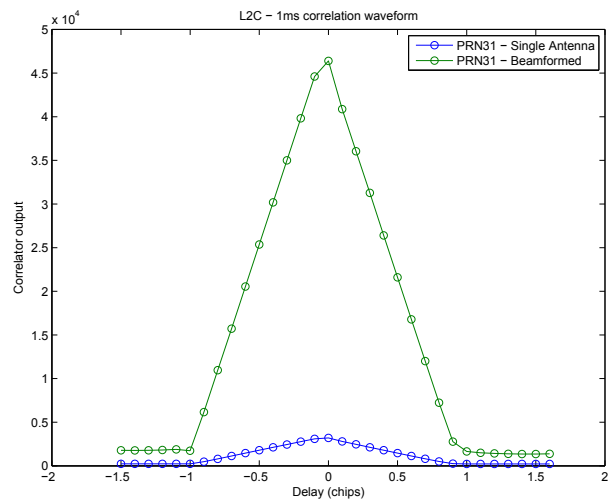


**Figure 9**. RSS of correlation waveform before and after L2 beamforming using 16 antennas.

*Flight Test*

The final verification was performed by installing the instrument in a Cessna aircraft (Figures 10 and 11) and flying off the California coast collecting reflections from the ocean surface.

*Experimental Setup*—The experimental setup for the Cessna flight was as follows:

- Real Time GNSS Receiver tracking direct signal
- Science processor
- Reconfigurable Digital Processor
- 4 Left-hand Circularly Polarized down-looking antennas
- 4 Right-hand Circularly Polarized down-looking antennas

For the first flight, the TOGA instrument was used in data recording mode, this means only IF samples were saved during flight and then processed offline after the flight.

**Figure 10**. Installation of equipment

**Figure 11**. 4 LHCP and 4 RHCP antennas installed on aircraft

*Reflected data*—The first flight test was successful and reflections were observed at both L1 and L5 frequencies. Delay doppler maps can be seen in Figures 12 and 13. Note how the wavefront arrives very abruptly and then (as delay increases), slowly tapers off - the shape of this waveform is directly correlated to surface roughness.

## 4. Conclusions

An overview of the TOGA instrument architecture as well as experimental test and flight data were given. The instrument is able to focus up to 8 simultaneous high-gain beams at 3 frequencies and direct these beams at specular reflection spots on the ocean surface as predicted by the science processor. With a 16 element array, a peak gain of greater than 20dB could be directed at multiple reflection spots.

The instrument operation was verified by conducting a series of test flights off the coast of California by collecting reflected

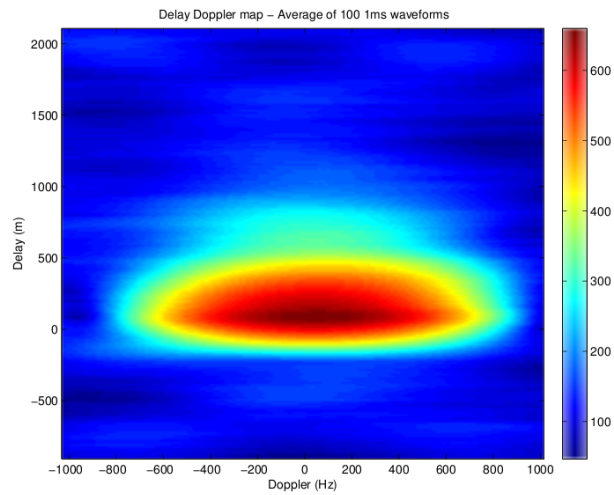


**Figure 12**. LHCP Delay Doppler map of ocean reflection for PRN28 at L1 C/A (Colormap shows 1s SNRv).

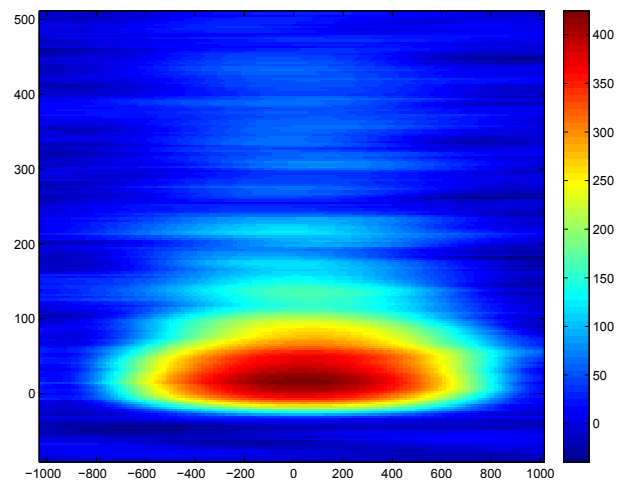


**Figure 13**. LHCP Delay Doppler map of ocean reflection for WAAS PRN138 at L5 (Colormap shows 1s SNRv).

signals with a set of right-hand and left-hand polarized antennas. The processed data was presented here as well as other experiments that were conducted to verify the correct operation of the instrument.

## Acknowledgments

This research was carried out at the Jet Propulsion Laboratory, California Institute of Technology, under a contract with the National Aeronautics and Space Administration.

## References

[1] M. Martin-Neira. A passive reflectometry and interferometry system (PARIS): Application to ocean altimetry. *ESA Journal*, 17, 1993.

[2] V.U. Zavorotny and A.G. Voronovich. Scattering of GPS signals from the ocean with wind remote sensing applications. *IEEE Transactions on Geoscience and Remote*

*Sensing*, 38(2):951, 2000.

[3] Dallas Masters. *Surface Remote Sensing Applications of GNSS Bistatic Radar: Soil Moisture and Aircraft Altimetry*. PhD thesis, University of Colorado at Boulder, 2004.

[4] M. Armatys, D. Masters, A. Komjathy, P. Axelrad, and J. L. Garrison. Exploiting GPS as a new oceanographic remote sensing tool. In *Insitute of Navigation GPS 2000*. ION, 2000.

[5] D.S. Masters, P. Axelrad, V. Zavorotny, S.J. Katzberg, and F. Lalezari. A passive GPS bistatic radar altimeter for aircraft navigation. In *Proceedings of the Institute of Navigation's ION GPS-2001*. ION, 2001.

[6] T.K. Meehan, S. Esterhuizen, G. W. Franklin, S. Lowe, T.N. Munson, D. Robison, D.J. Spitzmesser, J. Y. Tien, and L. E. Young. TOGA, a prototype for an optimal orbiting GNSS-R instrument. In *International Geoscience and Remote Sensing Symposium*. IEEE, 2007.

## BIOGRAPHY

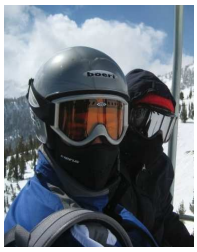

**Stephan Esterhuizen** B.S. (Computer Engineering), University of Colorado, Boulder, 2004; M.S. (Electrical Engineering), University of Colorado, Boulder, 2006. He joined JPL in 2006 where his primary task has been software and hardware development for the TOGA R&TD radio occultation and reflections instrument.